
Article:
Kernbach, Julius M., Thomas Yeo, B. T., Smallwood, Jonathan orcid.org/0000-0002-7298-2459 et al. (9 more authors) (2018) Subspecialization within default mode nodes characterized in 10,000 UK Biobank participants. Proceedings of the National Academy of Sciences of the United States of America. pp. 12295-12300. ISSN 1091-6490

https://doi.org/10.1073/pnas.1804876115

Subspecialization within default mode nodes characterized in 10,000 UK Biobank participants

Julius M. Kernbach[a], B. T. Thomas Yeo[b,c,d,e], Jonathan Smallwood[f], Daniel S. Margulies[g], Michel Thiebaut de Schotten[h,i], Henrik Walter[j], Mert R. Sabuncu[k,l,m], Avram J. Holmes[k,n,o,p], Alexandre Gramfort[q], Gaël Varoquaux[q], Bertrand Thirion[q], and Danilo Bzdok[a,q,r,1]

[a]Department of Psychiatry, Psychotherapy and Psychosomatics, RWTH Aachen University, 52072 Aachen, Germany; [b]Department of Electrical and Computer Engineering, Clinical Imaging Research Centre, Singapore Institute for Neurotechnology and Memory Networks Program, National University of Singapore (NUS), 117575 Singapore, Singapore; [c]NUS Graduate School for Integrative Sciences and Engineering, National University of Singapore, 119077 Singapore, Singapore; [d]Martinos Center for Biomedical Imaging, Massachusetts General Hospital, Harvard Medical School, Charlestown, MA 02129; [e]Centre for Cognitive Neuroscience, Duke-NUS Graduate Medical School, 169857 Singapore, Singapore; [f]Department of Psychology, York Neuroimaging Centre, University of York, York YO10 5DD, United Kingdom; [g]Centre National de la Recherche Scientifique, CNRS UMR 7225, Institut du Cerveau et de la Moelle Épinière, 75013 Paris, France; [h]Brain Connectivity and Behaviour Group, Frontlab, 75013 Paris, France; [i]Inserm, CNRS, Institut du Cerveau et la Moelle, Hôpital Pitié-Salpêtrière, Université Pierre et Marie Curie (UPMC), Université Paris 06, Sorbonne Universités, 75013 Paris, France; [j]Department of Psychiatry and Psychotherapy at Campus Charité Mitte, Charité-Universitätsmedizin Berlin, Corporate Member of Freie Universität Berlin, Humboldt-Universität zu Berlin, and Berlin Institute of Health, 10117 Berlin, Germany; [k]Athinoula A. Martinos Center for Biomedical Imaging, Massachusetts General Hospital, Harvard Medical School, Charlestown, MA 02129; [l]School of Electrical and Computer Engineering, Cornell University, Ithaca, NY 14853; [m]Nancy E. and Peter C. Meinig School of Biomedical Engineering, Cornell University, Ithaca, NY 14853; [n]Department of Psychology, Yale University, New Haven, CT 06520; [o]Department of Psychiatry, Yale University, New Haven, CT 06520; [p]Department of Psychiatry, Massachusetts General Hospital, Harvard Medical School, Boston, MA 02114; [q]Parietal Team, Institut National de Recherche en Informatique et en Automatique (INRIA), Neurospin, Commissariat à l'Energie Atomique (CEA-Saclay), Université Paris-Saclay, 91191 Gif-sur-Yvette, France; and [r]JARA-BRAIN, Jülich-Aachen Research Alliance, 52074 Aachen, Germany

Edited by Marcus E. Raichle, Washington University in St. Louis, St. Louis, MO, and approved October 15, 2018 (received for review March 21, 2018)

The human default mode network (DMN) is implicated in several unique mental capacities. In this study, we tested whether brain-wide interregional communication in the DMN can be derived from population variability in intrinsic activity fluctuations, gray-matter morphology, and fiber tract anatomy. In a sample of 10,000 UK Biobank participants, pattern-learning algorithms revealed functional coupling states in the DMN that are linked to connectivity profiles between other macroscopical brain networks. In addition, DMN gray matter volume was covaried with white matter microstructure of the fornix. Collectively, functional and structural patterns unmasked a possible division of labor within major DMN nodes: Subregions most critical for cortical network interplay were adjacent to subregions most predictive of fornix fibers from the hippocampus that processes memories and places.

systems neuroscience | high-level cognition | machine learning

The increasing cognitive sophistication apparent in primate evolution is frequently attributed to the expansion of association cortex (1), a substantial proportion of which is occupied by the "default mode network" (DMN) in humans (2). Invasive axonal tracing studies in association cortex areas in monkeys yield connectivity patterns similar to the human DMN (3). DMN regions also display late myelination during development (4), which is a common feature of areas that subserve higher cognitive functions (5, 6). The DMN is located at the top of a neural processing hierarchy with maximal distance, in structural and functional space, from primary visual and auditory areas (7). Finally, signals within DMN parts have been shown to contain "echoes" of neural systems from other large-scale networks (8). Together, these observations suggest that the involvement of the DMN in many sophisticated cognitive processes in humans may be anchored in the capacity of this system to provide a global mapping of brain dynamics. While emerging evidence supports a view of the DMN in widespread cortical coupling, it remains unknown how this network interfaces with other brain hubs to encode information from across the cortex.

A rich history of experimental evidence has shown that many high-level tasks recruit the DMN as a cohesive functional unit, including mental state attribution, moral dilemmas, and prospective thought (e.g., refs. 9 and 10). Despite much evidence for the DMN acting as a functional unit (cf. ref. 11), there is also evidence that its ability to interface with other cortical regions is closely related to particular parts of the system. For example, a functional dissociation may exist within the DMN between a midline core and a medial temporal subsystem, thought to closely interact with the hippocampus (12). Likewise, the right temporoparietal node was thought to be important for toggling between neural systems guided by internal information from memory and those processing external cues from the immediate environment (13). More generally, both analysis of task-evoked neural activity (12, 14) and individual-level analysis of intrinsic functional connectivity (15) suggest that the broader DMN may reflect a complex pattern of closely allied, yet functionally specific, interleaved neural systems. For example, within an individual, major nodes of the DMN were shown to embed parallel interdigitated systems that are currently impossible to resolve at the level of group averages (15). Together, this evidence highlights the possibility that important features of the DMN emerge

Significance

The default mode network (DMN) encompasses supramodal association areas involved in higher-order cognition. One speculation is that this neural system is important for brain-wide information flow. We tested this account by exploring whether DMN patterns are informative about functional coupling or structural associations in the rest of the brain. Our multimodal pattern analysis findings highlight how the DMN nodes are fractionated: In specific subnodes, gray-matter morphology was linked to fiber tracts from the hippocampus in the medial temporal limbic system. In adjacent subnodes, fluctuations in neural activity were linked to between-network connectivity shifts. Such a mosaic architecture may be a prerequisite for many of the roles the DMN may play in advanced cognitive processes.

Author contributions: J.M.K. and D.B. designed research; J.M.K. and D.B. performed research; B.T.T.Y., A.G., G.V., and B.T. contributed new reagents/analytic tools; J.M.K., J.S., D.S.M., M.T.d.S., H.W., M.R.S., A.J.H., and D.B. analyzed data; and J.M.K. and D.B. wrote the paper.

The authors declare no conflict of interest.

This article is a PNAS Direct Submission.

[1]To whom correspondence should be addressed. Email: danilo.bzdok@rwth-aachen.de.

This article contains supporting information online at www.pnas.org/lookup/suppl/doi:10.1073/pnas.1804876115/-/DCSupplemental.

Published online November 12, 2018.

from how information from other brain regions is expressed in different parts of the system.

Our population neuroscience study interrogated whether the role of the DMN in higher cognition may emerge from the ability to echo properties of remote large-scale brain networks (16). To this end, we capitalized on a recently available DMN atlas with subnode differentiation (13, 17–20). We reasoned that, if subspecialized regions within the DMN nodes act as relays that promote information from different parts of the neural hierarchy, this would facilitate information exchange between unisensory networks and other subordinate brain systems (8, 16). Using a multimodal brain imaging approach combining functional and structural measures of brain organization, we identified functional relationships between different DMN subnodes and major brain networks as well as their underlying anatomical architecture. Uniformly collected data from a large human population were systematically explored by multivariate pattern learning algorithms guided by our recent topographical DMN atlas.

Results

In the structural domain, we tested whether patterns within combined measurements of DMN volume [structural MRI (sMRI)] and axonal fiber bundles [diffusion MRI (dMRI)] would allow the identification of the white matter tracts with the strongest structural association with the DMN. We quantified generalizable patterns in DMN gray matter that inform about microstructural differences of white matter tracts (Johns Hopkins University atlas) across individuals. Gray matter volume was extracted in 32 DMN subregions per participant (Fig. 1) and used for pattern recognition algorithms [maximum-margin support vector regression (SVR)]. This approach could nominate the anatomical fiber tracts that were most predictive of gray matter volume estimates from within the DMN. The target diffusion measures included fractional anisotropy (FA, directional coherence), magnitude of diffusion, axial diffusivity, and radial diffusivity, as well as NODDI parameters, including tract complexity (OD), neurite density (ICVF), and extracellular water diffusion (ISOVF). After accounting for confounds (age, age^2, sex, their two-way interactions, head size, and body mass), pattern search models isolated structural associations between DMN and brain-wide anatomical tracts.

Comparing 48 candidate tracts, microstructural differences of three fornix-related fiber tracts were highly predictable based on gray matter differences within the DMN (Fig. 2), explaining up to 24% of population variance in this major hippocampus output pathway of the limbic system. These associations persisted across different diffusion parameters (*SI Appendix*, Fig. S2). Gray matter volume differences in DMN subregions were predictive of microstructure in a specific subset of anatomical tracts. The prediction accuracy for the common FA measure of white matter integrity ranged from $R^2 = 0.00$ to 0.24 across all tracts, with mean performance of 0.04 ± 0.04 (±SD) in unseen individuals (out-of-sample cross-validation). Across the atlas tracts, pattern detection performance was high for the fornix (Fig. 2 *A* and *B*) at an explained variance of 24% ($R^2 = 0.24$ ±0.03 SD across cross-validation splits), fornix fibers in the bilateral cres and stria terminalis (right: $R^2 = 0.09 \pm 0.01$; left: $R^2 = 0.08 \pm 0.02$), anterior corona radiata of the thalamus (left: $R^2 = 0.10 \pm 0.01$; right: $R^2 = 0.09 \pm 0.01$), posterior limb of the internal capsule (left: $R^2 = 0.08 \pm 0.03$; right: $R^2 = 0.06 \pm 0.02$), and superior frontal–occipital fasciculus (left: $R^2 = 0.12 \pm 0.02$; right: $R^2 = 0.05 \pm 0.02$).

We then examined which particular DMN subregions show strongest predictive associations with fornix microstructure differences (Fig. 2*C*). Robust contributions to this predictive relationship (bagging) were apparent in the right and left temporoparietal junctions (TPJs) [$\text{weight}_{\text{R\_TPJ-1}} = -0.61 \pm 0.04$ (SD of bootstrap distributions), $\text{weight}_{\text{R\_TPJ-2}} = 0.75 \pm 0.07$, $\text{weight}_{\text{L\_TPJ-1}} = -0.25 \pm 0.06$, and $\text{weight}_{\text{L\_TPJ-2}} = -0.18 \pm 0.07$], medial portions of left ventromedial prefrontal cortex (vmPFC; $\text{weight}_{\text{L\_vmPFC-1}} = 0.17 \pm 0.03$, $\text{weight}_{\text{L\_vmPFC-3}} = -0.64 \pm 0.07$), left middle temporal gyrus (MTG) ($\text{weight}_{\text{L\_MTG-2}} = -0.32 \pm 0.05$, $\text{weight}_{\text{L\_MTG-3}} = 0.31 \pm 0.04$), and in the dorsal posterior cingulate and retrosplenial cortex ($\text{weight}_{\text{PMC-3}} = -0.13 \pm 0.09$, $\text{weight}_{\text{PMC-4}} = 0.18 \pm 0.03$). We conclude that especially the right TPJ, its left counterpart, the left vmPFC, and posterior parts of the left MTG, as well as the posterior cingulate and retrosplenial midline were found most relevant among DMN gray matter patterns that predict fornix microstructure.

In the functional domain, we sought to identify connectivity patterns in the DMN that explain its correspondence with patterns of distributed neural activity. Topographical segregation of the DMN was obtained from the group-defined DMN atlas with 32 subregions (Fig. 1), while population-average definitions of 21 spatiotemporal networks were provided by UK Biobank. Canonical correlation analysis (CCA) was a natural choice of method to jointly decompose the functional relationships among DMN subregions and those between major networks across individuals. After confound removal (age, age^2, sex, their two-way interactions, head motion, head size, and body mass), this doubly multivariate analysis extracted coherent patterns of connectivity modulation. These population "modes" provided a rich summary of how functional coupling changes in the segregated DMN covary with functional coupling changes of large-scale networks.

To control the amount of detail in CCA modeling, we obtained family-wise error-corrected *P* values for all modes by permutation testing analogous to previous research (21, 22). Among all estimated components, 19 modes of covariation were highly statistically significant at $P_{\text{corrected}} < 0.001$ (Fig. 3*B*), in line with previous CCA analyses on UK Biobank participants (21). Each isolated DMN–networks mode captured a distinct source of covariation that together were mutually uncorrelated. Collectively, this analysis shows that neural

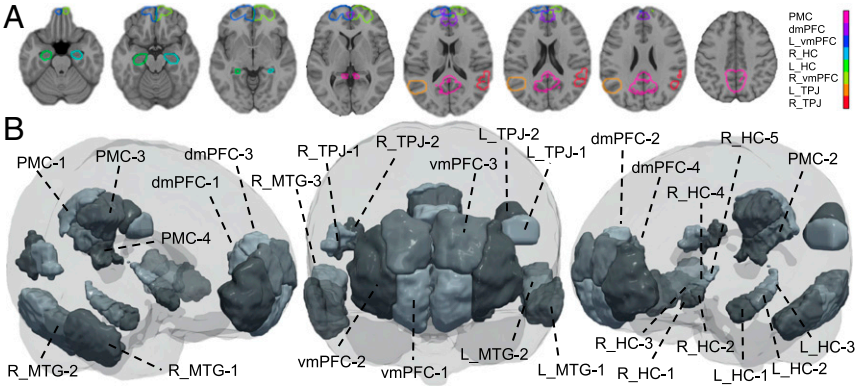

Fig. 1. Target atlas definition for the DMN. (*A*) DMN with its major nodes as commonly studied in neuroimaging. (*B*) A DMN division into 32 subregions provided the basis for all present investigations, including four subregions in the dmPFC, six in the vmPFC, four in the PMC, six in the bilateral MTG, four in the bilateral TPJ, and eight in the bilateral HC from a recent quantitative atlas (13, 17–20, 47, 48). The 32 DMN compartments allowed analyzing the brain-wide structural and functional correspondence at a fine-grained scale of inquiry (see *SI Appendix*, Fig. S1). All subregion definitions are open for inspection and reuse (https://neurovault.org/collections/3434/). L/R, left/right.

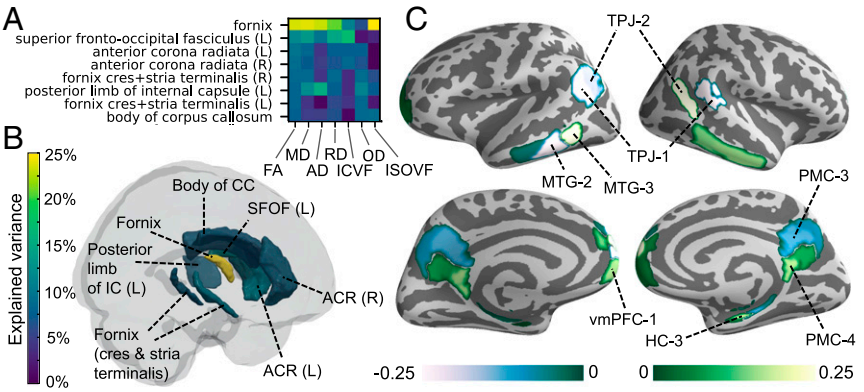

Fig. 2. DMN subregion structure is predictive of fornix fibers from the hippocampus. DMN gray matter volumes exposed generalizable patterns that explain white matter tract variability. Among 48 anatomical fiber bundles, three highly predictable tracts carried fornix-related fibers, a major hippocampus output pathway from the limbic system, with 24%, 9%, and 8% explained population variance. (*A*) Prediction accuracy (R^2 scores) for the eight most robustly inferred fiber tracts for various diffusion MRI measures, starting from highest estimated performance in yet-to-be-observed individuals. (*B*) Anatomical tracts with strongest DMN association (color indicates out-of-sample R^2). (*C*) Prominent predictive association with fornix microstructure (mean FA) was located in the bilateral TPJs, medial parts of left vmPFC, posterior parts of left MTG, and right HC, as well as dorsal posterior cingulate (PMC-3) and retrosplenial (PMC-4) cortex. Subregions in green–yellow (blue) increased (decreased) volume together with fornix FA across individuals (*SI Appendix*, Fig. S2).

activity patterns within the DMN are related to distributed patterns of large-scale networks.

Next, we examined whether these modes of covariation were localized in particular DMN subregions. To aid interpretation, we visualized where average changes of coupling between DMN subregions were most related to between-network coupling changes. This summary highlights the DMN subregions most consistently associated with changes of global network connectivity across all significant modes (Fig. 3*A*). Analogous to previous research (22), the cumulative increases and decreases of DMN subregion connectivity were examined separately.

Each major DMN node was found to have a subregion dedicated to overall network coupling. Specific subregions within a given DMN node tended to show either mostly increased or mostly decreased functional relationships that coherently cooccur with network coupling shifts. The lateral portion of the vmPFC (bilateral vmPFC-2) as well as the anterior TPJs (bilateral TPJ-1), anterior MTGs (bilateral MTG-1), and precuneus of the posterior medial cortex (PMC-1) increased in neural coupling, on average, in the context of global network communication. In contrast, mostly decreased coupling was observed in many adjacent subregions, including the left and right medial portions of the vmPFC (vmPFC-1/3), posterior TPJs (TPJ-2), posterior MTGs (MTG-3), and ventral posterior cingulate cortex (PMC-2/4). Conversely, we examined the overall connectivity changes of major brain networks (separately for positive and negative shifts) that most related to within-DMN connectivity changes across all modes (Fig. 3*C*). In contrast to the DMN subregions, we found a high degree of spatial overlap between the brain networks that were subject to connectivity changes. The concurrent network coupling changes included the somatomotor cortex, thalamus, frontal eye field (FEF), dorsolateral prefrontal cortex (dlPFC), anterior insula (AI), intraparietal sulcus (IPS), anterior cingulate cortex (ACC) and posterior cingulate cortex (PCC), as well as secondary associative visual (e.g., MT/V5) and auditory areas. These regions are often described as "task-positive" brain networks (23).

As a recurring theme across the 19 functional modes of population covariation, several coupling profiles showed one DMN subregion dominating intra-DMN connectivity in the context of broad network reconfiguration. The bilateral anterior TPJs (TPJ-1) were found to dominate in the DMN–networks correspondence (Fig. 4), as these two subregions showed prominent coupling increases in three modes. In the first mode of DMN–networks correspondence ($r = 0.83$), both anterior TPJs were increasingly coupled with most other DMN subregions, and the subregions of the left and right hippocampus increased their coupling among each other. Concurrently, at the global network level, the DMN was disengaged from the saliency network. Further, the somatomotor networks were more coupled among each other, increased in coupling with the medial temporal lobe and superior temporal gyrus, as well as decreased in coupling with the cerebellum and basal ganglia. In mode 5 ($r = 0.72$), the right anterior TPJ showed increased coupling with most DMN subregions, in particular with the posteromedial cortex (PMC-1/2/3/4), midline parts of the ventromedial prefrontal cortex (vmPFC-1/3) and dorsomedial prefrontal cortex (dmPFC-1/2/3/4). Concurrently, the overall DMN had decreased coupling with the saliency network and with the left dorsal attention network in favor of the right dorsal attention network. Finally, in mode 8 ($r = 0.68$), the left anterior TPJ was up-regulated in coupling with many DMN subregions, in particular with the precuneus (PMC-1), ventral and dorsal posterior cingulate cortex (PMC-2/3), and retrosplenial cortex (PMC-4). In this context, the entire DMN was decoupled from the right dorsal attention network, which, in

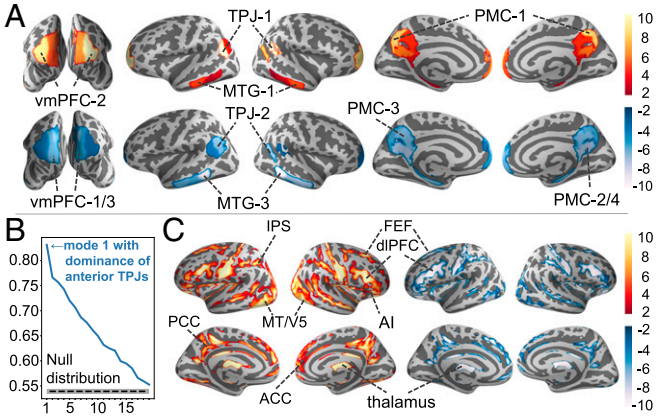

Fig. 3. Functional coupling among DMN subregions is associated with between-network interplay. Summarizing the 19 population modes for display reveals how functional connectivity changes in the DMN explain brain-wide connectivity changes between major networks (*SI Appendix*, Figs. S3–S6). (*A*) Biggest positive vs. negative cumulative modulation of connectivity between subregions is apparent in the anterior vs. posterior TPJs, lateral vs. medial portions of the vmPFC, anterior vs. posterior MTG, and precuneus vs. posterior cingulate midline. DMN subregions in hot (cool) colors are related to increases (decreases) of baseline connectivity strength that accompany specific network connectivity shifts. (*B*) Importance of the 19 modes measured by Pearson's correlation between canonical variates (blue), all statistically significant at P value < 0.001. (*C*) Biggest positive and negative cumulative network modulations were spatially overlapping. Of note is that the DMN subregions with high modulation weights across modes are mostly located outside of the brain networks with the most recruitment changes.

NEUROSCIENCE

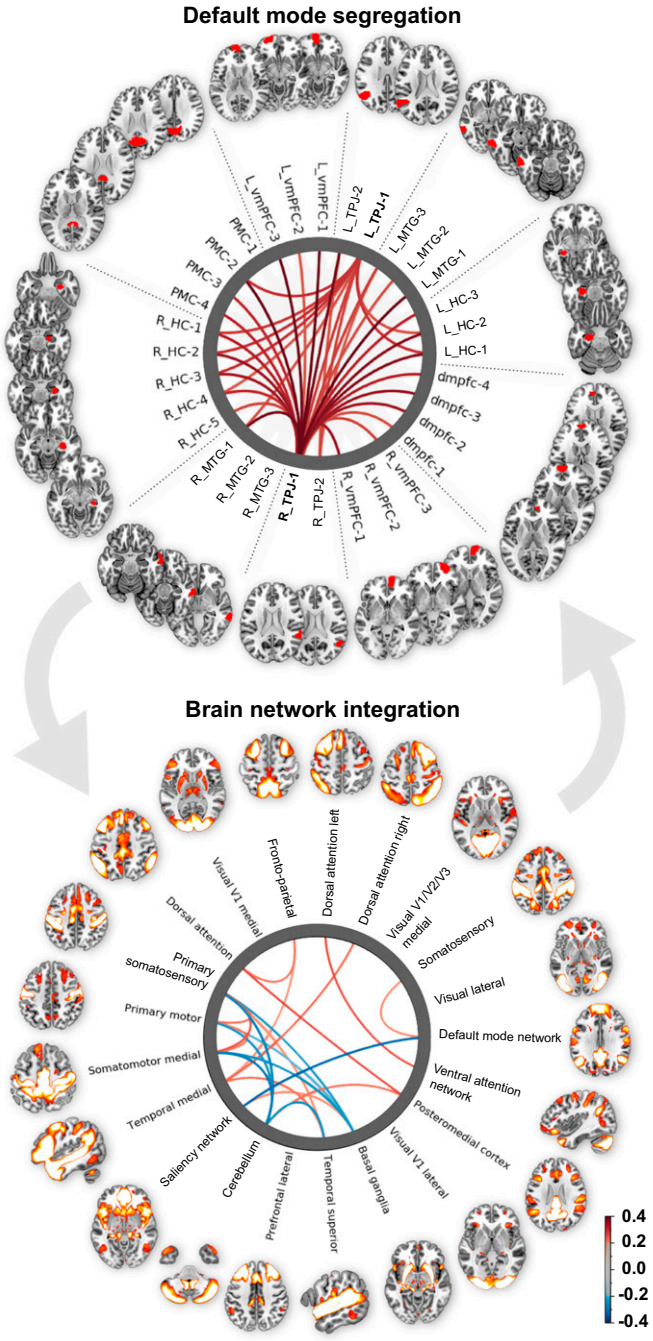

Fig. 4. Functional coupling shifts of the statistically strongest DMN–networks mode, depicting the single most important mode among 19 linked dimensions of within-DMN connectivity (*Top*) and between-network connectivity (*Bottom*). Increased coupling of anterior TPJs with other DMN subregions was estimated to be dominantly involved in connectivity shifts of large-scale networks. Such partial-correlation analyses have become a standard to focus on immediate coupling relationships between brain regions (49). It is, however, important to keep in mind that this type of connectivity analysis is susceptible to noise and does not permit statements about directional or causal functional influences (50).

turn, increased in functional connectivity with the left dorsal attention network.

The functional coupling theme of a specific subregion driving the DMN–networks correspondence was also observed in other modes for the precuneus (PMC-1) and lateral portion of the ventromedial prefrontal DMN (vmPFC-2) (*SI Appendix*, Figs. S3–S6). In the second most important mode (r = 0.77), the precuneus showed increased coupling with most DMN subregions. Concurrently, at the network integration level, the DMN disengaged with the saliency network, analogous to mode 1, and showed decreased coupling with somatosensory cortices, dlPFC, dorsal attention networks, and lateral visual cortex. In mode 9 (r = 0.66), the lateral subregions of the right vmPFC similarly increased coupling with most DMN subregions. In this mode, the ventral attention network was disengaged with the dorsal attention network, posteromedial cortices, and dlPFC, while the saliency network was decoupled from parietal cortices and was increased in coupling with dorsal attention network and dlPFC. We conclude that DMN subregions in the anterior TPJ, precuneus, and lateral vmPFC appear to play particularly important roles related to the functional interplay between large-scale networks.

We confirmed evidence from intrinsic coupling fluctuations by inducing "virtual DMN lesions" and computing a series of perturbed CCA models. This analysis tactic allowed the determination of subregions most critical across all 19 DMN–networks modes (*SI Appendix*, Figs. S7 and S8). Lower-correlation results indicate that removing that region leads to a quite different result, thus emphasizing the important influence of a "deleted" subregion in the original CCA decompositions. The obtained importance ranking substantiated the relevant connectivity links from particular DMN subregions: the anterior TPJs [right TPJ-1 $r = 0.15 \pm 0.16$ (SD of bootstrap distributions), left TPJ-1 $r = 0.46 \pm 0.17$], precuneus (PMC-1 $r = 0.09 \pm 0.12$), and lateral vmPFC (left vmPFC-2 $r = 0.26 \pm 0.18$, right vmPFC-2 $r = 0.44 \pm 0.17$). The analysis showed that neural signals in these subregions, rather than the DMN as a whole, were most important in the model's ability to determine functionally related patterns in the interactions between other brain networks.

Discussion

Over the last 15 y, understanding the functional significance of the DMN has become an important topic in neuroscience. Although the DMN is often characterized as a cohesive brain system, increasing evidence has begun to challenge this view (8, 12, 14–16, 24, 25). A recent study has shown heterogeneity at the level of an individual (15), and we revisited this question from the perspective of a large-scale population study. Combining a high-throughput biomedical dataset with innovative data analytics, we used multimodal evidence to outline an organizational fragmentation of major DMN nodes. We characterized neighborhoods of structurally and functionally distinct yet complementary submodules within major nodes of the DMN, which interfaced with other brain regions in unique manners. We consider the relevance of these results for our understanding of the hypothesized role of the DMN in broader cortical dynamics.

In brain structure, we used pattern extraction algorithms to identify statistically rigorous links between DMN gray matter (sMRI) and white matter tract properties (dMRI)—two types of brain imaging usually studied separately. Our multimodal approach determined whether volume differences of DMN subregions are informative about microstructural features of axonal fiber bundles. Among 48 examined anatomical tracts, fornix fibers had the strongest association with DMN gray matter patterns, explaining up to 24% of this tract's population variability. As with other small fiber tracts analyzed by diffusion imaging with tract-based spatial statistics (26), it is challenging to completely exclude the possibility that mild partial volume effects have influenced our fornix–DMN association results. Cerebrospinal fluid contamination may be alleviated by more sophisticated voxel-by-voxel correction techniques (27). Nevertheless, our predictive association of DMN gray matter with fornix fiber bundles was robust in 10,000 individuals and appears to fill an important gap in the neuroscience literature.

The fornix serves as backbone of the limbic system and main output tract of the hippocampus into the cortex. This tract guides axonal fibers from structures in the medial temporal space memory system to communicate with cortical association areas (28) by intermediates such as the anterior thalamic radiation.

Consistent with our demonstrated population association between the fornix and the vmPFC, probabilistic diffusion tractography in humans and monkeys showed that fornix-carried fiber bundles play a prominent role in connections of the hippocampus with the vmPFC (29). Moreover, hippocampal lesions in six neurological patients led to significant FA reductions in the fornix but no other white matter tracts, functional connectivity alterations in the DMN, and episodic memory impairments (30). Similarly, in patients with posttraumatic amnesia, functional connectivity between the medial temporal lobe and the posteromedial DMN correlated with associative memory performance and information processing speed (31). Building on these studies, our work leverages large-scale population data to highlight the relevance of the hippocampal–neocortical pathways in the functioning of the DMN and suggests that subregions, such as vmPFC and TPJ, which are most selective structural predictors of fornix anatomy, may be particularly important in this process.

In animals, single-cell recordings in the hippocampus have confirmed the existence of neuron assemblies involved in retrospective and prospective processing of spatial contexts, experienced events, and their complicated interaction (32). In fact, the limbic medial temporal lobe, including the hippocampus, is believed to be particularly prominent in the modulation by theta-band oscillations (32). Accumulating evidence from animal experiments suggests oscillatory synchrony in the theta regime to subserve neuronal coding in the hippocampus, including previously experienced, ongoing, and upcoming events, and its partners in the limbic system, as well as hippocampal long-distance communication with neocortical partners (32). Indeed, specific electrophysiological signals recorded in the monkey hippocampus were recently reported to trigger distributed neural activity changes in the DMN, but not other common cortical networks (33).

In humans, hippocampal–prefrontal oscillations in the theta band have also been linked to memory processes (34), and coordination between the prefrontal and temporoparietal DMN was shown to largely underlie theta-mediated oscillatory coupling (35). Congruently, seeding spontaneous fMRI activity fluctuations in the human hippocampus revealed signal reverberations in the major DMN nodes, which suggests an "ongoing functional relationship" (36). Further, quantitative metaanalyses of human neuroimaging tasks have established extensive spatial overlap in the DMN for neural activity increases during autobiographical memory retrieval, spatial navigation, anticipation of future events, and mind wandering (10)—all similar to findings from invasive experiments in the animal hippocampus. Finally, hippocampal functional connectivity with the medial prefrontal cortex was associated with patterns of thought that emphasize mental time travel (37). Our study builds on these findings by providing evidence at the level of the population that, compared with other tracts, individual differences in fornix white matter microstructure are particularly associated with gray matter differences within the DMN. One possibility is that this structural association reflects the underlying functional link between hippocampal systems and those within the DMN.

In the functional domain, we used CCA to explore whether patterns of functional coupling among DMN subregions were linked to functional connectivity changes between other macroscopical networks. Building on evidence of the DMN nodes as convergence zones of neural activity from the broader cortical system (7, 38), we used CCA to quantify how functional coupling shifts inside our group-defined DMN relate to functional coupling shifts between major brain networks distributed across the entire cortex. Our pattern search analysis highlighted major DMN nodes as possible hubs of interplay between distributed functional networks (16), providing evidence for a role of this system in two levels of brain organization usually studied in isolation: functional integration of common cortical networks and functional segregation of local specialized regions.

Our CCA analysis highlighted the right anterior TPJ of the DMN as a potential key player in mediating the functional interplay between brain networks, consolidating this previously proposed role of the DMN node (13). Among 32 candidate regions in our DMN atlas, this subregion in the inferior parietal lobe turned out to be most selectively important within DMN–networks coupling in the population mode that explained the most variance in DMN–networks interplay. Coupling increases of the right anterior TPJ, and its homologous subregion on the left, were related to down-regulated coupling between the DMN and the saliency network as well as up-regulated coupling among somatomotor networks. Our study adds to previous observations that several functional network patterns of correlation and anticorrelation spatially overlap in DMN regions (39). In particular, our results suggest that the apparent antagonism between the DMN and brain systems more closely linked to perception and action (7) may be related to the role of the anterior TPJ in the right and left hemisphere (13). This pattern of functional associations is consistent with the importance of the TPJ in describing global cortical dynamics, as these states likely depend on bringing together patterns of neural information processing.

At the most general level, our study suggests that global DMN dynamics may emerge from the combination of nodes that cooperate yet can have distinct functional relationships to other brain areas. Our analysis complements an emerging view which emphasizes the importance of flexibility in the dynamics of canonical brain networks (40). Indeed, our supplementary analyses (see *SI Appendix*, Figs. S9–S11) are in line with a whole-brain graph analysis (41) that reported individuals with higher IQ to have shorter path length in nodes of the DMN, which the authors interpreted as improved global efficiency of information transfer across networks. Hubs underlying general network control have been mainly identified in the DMN (38). Our analysis suggests that these hubs may make different contributions to cortical functioning.

There are a number of caveats that should be borne in mind while considering our results obtained at the population level. First, since we chose a DMN subregion atlas, our study aimed at insight into how segregation and integration unfold within this brain phenomenon. However, we do not provide insight into how these observations fit into views of other networks or neural systems. It will be important to examine how network fragmentation approaches may play out in other cortical networks, such as the frontoparietal network. Second, we explored how the group-defined DMN links to the rest of the brain, identifying patterns of organization within this system through their variation across 10,000 individuals. While our analysis highlights the topographic location in which signals within the group-defined DMN possibly carry information about neural processing distributed across the cortex, there is likely to be important information that can be gained by exploring this problem at a more fine-grained level. Recent evidence suggests the existence of parallel interdigitated networks that together make up what is commonly labeled as DMN after averaging across individuals (15).

Despite the considerable methodological differences between this previous participant level and our population level results, there are nonetheless certain similarities. In particular, the DMN subtype A proposed by Braga and Buckner (15) appears to extend toward more posterior regions of the TPJ (similar to TPJ-2 in our study), more ventromedial prefrontal cortex (vmPFC-1/3 here), and ventral/retrosplenial PCC (PMC-2/4). In contrast, the DMN subtype B appears localized to the anterior TPJs (TPJ-1 here), more dorsomedial prefrontal cortex (dmPFC-1/2/3/4 here), and dorsal PCC (PMC-3 here). These similarities are noteworthy given the diverging methodology in the two studies.

It is the objective of a population neuroscience study to target major principles of brain organization. We highlight those regions of the DMN that are most robustly involved in patterns of within- and between-network interactions. However, both the hard boundaries of our DMN definition and their deviations through the registration process (cf. refs. 42–44) may obscure certain aspects of the underlying function (15, 42, 45). In

particular, it is unclear in our current analyses whether DMN subregions highlight areas with homogeneous patterns of neural activity with a unified functional purpose, or whether they describe areas where the interleaving of different neural function occurs, which may represent "a generalized anatomic mechanism for processing information from two or more cortical sources in the central nervous system" (ref. 46, p. 792).

In conclusion, our results suggest spatial proximity between subregions in major DMN nodes that offer complementary structural and functional properties. Such topographic organization could provide a scaffold for communication between subregions that track unique aspects of whole-brain functional modes. We identified cortical subregions of the DMN that were closely allied to fornix microarchitecture, which, we speculate, may perhaps be related to processing information from the hippocampus in the medial temporal lobe as well as other DMN subregions that were important in explaining functional coupling shifts between major cortical networks. This mosaic biological design, we further speculate, may contribute to resolving competing requirements of modular functional specialization with between-network interplay via long-distance connections. While the DMN has repeatedly been shown to be placed at the heart of the brain network hierarchy (3, 7, 38), the DMN is itself composed of distributed modules, each of which embodies distinct submodules (8, 16, 24).

Materials and Methods

The 500,000 UK Biobank participants were recruited from across Great Britain. All participants provided informed consent. The present analyses were conducted under UK Biobank application number 25163. Further information on the consent procedure can be found here (biobank.ctsu.ox.ac.uk/crystal/field.cgi?id=200). Our study involved brain imaging from 10,129 individuals, 47.6% males and 52.4% females, aged 40 y to 69 y, to detail the neurobiological properties of the DMN by means of T1-weighted MRI (sMRI), dMRI, and resting-state functional MRI (fMRI). Jointly analyzing gray matter volume (sMRI) and white matter microstructure (dMRI) allowed testing whether interindividual differences in DMN volume are linked to variability in fiber bundle microstructure. The DMN subregion volumes of each subject provided the input data for pattern learning analyses based on maximum–margin linear SVR to assess predictability of water diffusion characteristics of 48 white matter tracts. Functional connectivity measures among DMN subregions were derived by computing the partial correlations between their neural activity fluctuations (fMRI), guided by the DMN atlas. Topographical definitions of 21 common large-scale networks were used with the network analysis tool from FSL (FSLNets) to compute partial correlations between every pair of networks.

ACKNOWLEDGMENTS. We thank the UK Biobank participants for their voluntary commitment. We thank Denis Engemann, Kevin Anderson, and Demian Wassermann for advice on data processing. B.T.T.Y. was supported by the Singapore National Research Foundation Fellowship (Class of 2017). D.B. was funded by the Deutsche Forschungsgemeinschaft Grants BZ2/2-1, BZ2/3-1, BZ2/4-1, and IRTG2150 and Amazon Web Service cloud computing grants.

1. Van Essen DC, Dierker DL (2007) Surface-based and probabilistic atlases of primate cerebral cortex. *Neuron* 56:209–225.
2. Raichle ME, et al. (2001) A default mode of brain function. *Proc Natl Acad Sci USA* 98:676–682.
3. Buckner RL, Krienen FM (2013) The evolution of distributed association networks in the human brain. *Trends Cogn Sci* 17:648–665.
4. Flechsig P (1920) *Anatomie des menschlichen Gehirns und Rückenmarks auf myelogenetisch Grundlage* (Thieme, Leipzig, Germany).
5. Yakovlev PL, Lecours AR (1967) The myelogenetic cycles of regional maturation of the brain. *Regional Development of the Brain in Early Life*, ed Minkowski A (FA Davis, Philadelphia), pp 3–70.
6. Sowell ER, et al. (2003) Mapping cortical change across the human life span. *Nat Neurosci* 6:309–315.
7. Margulies DS, et al. (2016) Situating the default-mode network along a principal gradient of macroscale cortical organization. *Proc Natl Acad Sci USA* 113:12574–12579.
8. Leech R, Braga R, Sharp DJ (2012) Echoes of the brain within the posterior cingulate cortex. *J Neurosci* 32:215–222.
9. Bzdok D, et al. (2012) Parsing the neural correlates of moral cognition: ALE meta-analysis on morality, theory of mind, and empathy. *Brain Struct Funct* 217:783–796.
10. Spreng RN, Mar RA, Kim AS (2009) The common neural basis of autobiographical memory, prospection, navigation, theory of mind, and the default mode: A quantitative meta-analysis. *J Cogn Neurosci* 21:489–510.
11. Buckner RL, Andrews-Hanna JR, Schacter DL (2008) The brain's default network: Anatomy, function, and relevance to disease. *Ann N Y Acad Sci* 1124:1–38.
12. Andrews-Hanna JR, Reidler JS, Sepulcre J, Poulin R, Buckner RL (2010) Functional-anatomic fractionation of the brain's default network. *Neuron* 65:550–562.
13. Bzdok D, et al. (2013) Characterization of the temporo-parietal junction by combining data-driven parcellation, complementary connectivity analyses, and functional decoding. *Neuroimage* 81:381–392.
14. Yeo BT, et al. (2015) Functional specialization and flexibility in human association cortex. *Cereb Cortex* 25:3654–3672.
15. Braga RM, Buckner RL (2017) Parallel interdigitated distributed networks within the individual estimated by intrinsic functional connectivity. *Neuron* 95:457–471.e5.
16. Braga RM, Sharp DJ, Leeson C, Wise RJ, Leech R (2013) Echoes of the brain within default mode, association, and heteromodal cortices. *J Neurosci* 33:14031–14039.
17. Bzdok D, et al. (2016) Left inferior parietal lobe engagement in social cognition and language. *Neurosci Biobehav Rev* 68:319–334.
18. Eickhoff SB, Laird AR, Fox PT, Bzdok D, Hensel L (2016) Functional segregation of the human dorsomedial prefrontal cortex. *Cereb Cortex* 26:304–321.
19. Bzdok D, et al. (2015) Subspecialization in the human posterior medial cortex. *Neuroimage* 106:55–71.
20. Ray KL, et al. (2015) Co-activation based parcellation of the human frontal pole. *Neuroimage* 123:200–211.
21. Miller KL, et al. (2016) Multimodal population brain imaging in the UK Biobank prospective epidemiological study. *Nat Neurosci* 19:1523–1536.
22. Smith SM, et al. (2015) A positive-negative mode of population covariation links brain connectivity, demographics and behavior. *Nat Neurosci* 18:1565–1567.
23. Fox MD, et al. (2005) The human brain is intrinsically organized into dynamic, anticorrelated functional networks. *Proc Natl Acad Sci USA* 102:9673–9678.
24. Leech R, Kamourieh S, Beckmann CF, Sharp DJ (2011) Fractionating the default mode network: Distinct contributions of the ventral and dorsal posterior cingulate cortex to cognitive control. *J Neurosci* 31:3217–3224.
25. Mayer JS, Roebroeck A, Maurer K, Linden DE (2010) Specialization in the default mode: Task-induced brain deactivations dissociate between visual working memory and attention. *Hum Brain Mapp* 31:126–139.
26. Smith SM, et al. (2006) Tract-based spatial statistics: Voxelwise analysis of multi-subject diffusion data. *Neuroimage* 31:1487–1505.
27. Metzler-Baddeley C, O'Sullivan MJ, Bells S, Pasternak O, Jones DK (2012) How and how not to correct for CSF-contamination in diffusion MRI. *Neuroimage* 59:1394–1403.
28. Cavada C, Compañy T, Tejedor J, Cruz-Rizzolo RJ, Reinoso-Suárez F (2000) The anatomical connections of the macaque monkey orbitofrontal cortex. A review. *Cereb Cortex* 10:220–242.
29. Croxson PL, et al. (2005) Quantitative investigation of connections of the prefrontal cortex in the human and macaque using probabilistic diffusion tractography. *J Neurosci* 25:8854–8866.
30. Henson RN, et al. (2016) The effects of hippocampal lesions on MRI measures of structural and functional connectivity. *Hippocampus* 26:1447–1463.
31. De Simoni S, et al. (2016) Disconnection between the default mode network and medial temporal lobes in post-traumatic amnesia. *Brain* 139:3137–3150.
32. Buzsáki G (2006) *Rhythms of the Brain* (Oxford Univ Press, Oxford).
33. Kaplan R, et al. (2016) Hippocampal sharp-wave ripples influence selective activation of the default mode network. *Curr Biol* 26:686–691.
34. Backus AR, Schoffelen J-M, Szebényi S, Hanslmayr S, Doeller CF (2016) Hippocampal-prefrontal theta oscillations support memory integration. *Curr Biol* 26:450–457.
35. Hipp JF, Siegel M (2015) BOLD fMRI correlation reflects frequency-specific neuronal correlation. *Curr Biol* 25:1368–1374.
36. Vincent JL, et al. (2006) Coherent spontaneous activity identifies a hippocampal-parietal memory network. *J Neurophysiol* 96:3517–3531.
37. Karapanagiotidis T, Bernhardt BC, Jefferies E, Smallwood J (2017) Tracking thoughts: Exploring the neural architecture of mental time travel during mind-wandering. *Neuroimage* 147:272–281.
38. Gu S, et al. (2015) Controllability of structural brain networks. *Nat Commun* 6:8414.
39. Smith SM, et al. (2012) Temporally-independent functional modes of spontaneous brain activity. *Proc Natl Acad Sci USA* 109:3131–3136.
40. Cole MW, Yarkoni T, Repovš G, Anticevic A, Braver TS (2012) Global connectivity of prefrontal cortex predicts cognitive control and intelligence. *J Neurosci* 32:8988–8999.
41. van den Heuvel MP, Stam CJ, Kahn RS, Hulshoff Pol HE (2009) Efficiency of functional brain networks and intellectual performance. *J Neurosci* 29:7619–7624.
42. Laumann TO, et al. (2015) Functional system and areal organization of a highly sampled individual human brain. *Neuron* 87:657–670.
43. Steinmetz H, Seitz RJ (1991) Functional anatomy of language processing: Neuroimaging and the problem of individual variability. *Neuropsychologia* 29:1149–1161.
44. Kong R, et al. (June 6, 2018) Spatial topography of individual-specific cortical networks predicts human cognition, personality, and emotion. *Cereb Cortex*, 10.1093/cercor/bhy123.
45. Gordon EM, et al. (2017) Precision functional mapping of individual human brains. *Neuron* 95:791–807.e7.
46. Selemon LD, Goldman-Rakic PS (1985) Longitudinal topography and interdigitation of corticostriatal projections in the rhesus monkey. *J Neurosci* 5:776–794.
47. Robinson JL, et al. (2015) Neurofunctional topography of the human hippocampus. *Hum Brain Mapp* 36:5018–5037.
48. Schaefer A, et al. (2018) Local-global parcellation of the human cerebral cortex from intrinsic functional connectivity MRI. *Cereb Cortex* 28:3095–3114.
49. Smith SM, et al. (2011) Network modelling methods for FMRI. *Neuroimage* 54:875–891.
50. Friston KJ (2011) Functional and effective connectivity: A review. *Brain Connect* 1:13–36.